Heat Transfer from a Circulating Fluidized Bed to Membrane Waterwall Surfaces

Average and local heat transfer coefficients were measured for transfer from circulating fluidized beds of sand particles (mean size 188 and 356 μm) to two water-cooled membrane wall surfaces located on one face of a 152 mm square by 7.3 m tall column. The measurements cover a range of superficial gas velocities from about 4 to 7 m/s, suspension densities from about 8 to 130 kg/m^3, suspension temperatures from 150 to 400°C, and secondary-to-primary air ratios of 0 to 1.5. Heat transfer coefficients, averaged over a 1.53 m length of the membrane waterwall surfaces, depend strongly on suspension density, but show almost no separate dependence on gas velocity, bed temperature, or secondary-to-primary air ratio for the conditions studied. For the surface nearest the top of the unit, the coefficient decreases with distance measured downward from the top, suggesting that particles travel downward along the surface. As a result, averaged coefficients are lower and the influence of particle size is less than for previously reported circulating fluidized bed heat transfer measurements where miniature heat transfer surfaces were employed.

R. L. Wu, C. J. Lim, Jamal Chaouki, J. R. Grace
Department of Chemical Engineering
The University of British Columbia
Vancouver, BC, Canada V6T 1W5

Introduction

Circulating fluidized beds (CFB's) are beginning to capture a major fraction of the market for large-scale steam boilers because of their ability to burn a wide variety of solid fuels with low pollutant emissions and good turndown. Knowing how the heat transfer coefficient between gas-solid suspensions and cooling surfaces varies with operating conditions is critical to the operation of CFB boilers since turndown is commonly achieved by varying the suspension density in the unit (Kobro and Brereton, 1986). Heat removal from circulating fluidized bed boilers is usually provided by exposed membrane waterwalls bounding the combustion region above ports which introduce secondary air. In order to specify the total surface area and the turndown characteristics of these cooling surfaces, information is needed on circulating-bed-to-surface heat transfer coefficients. For large units, membrane surfaces may also be suspended in the interior from above or from the side, and it is again essential to be able to estimate heat transfer coefficients.

Despite the importance of being able to predict heat transfer coefficients in circulating fluidized beds, experimental data are few in number. Moreover, most of the available data (Grace, 1986) are for very small heat transfer surfaces suspended within the interior of small-scale columns operated at room temperature. In this paper, we present data on heat transfer to membrane wall surfaces on the wall of a pilot-scale circulating fluidized bed unit operated at superficial gas velocities up to 7 m/s, solids fluxes from 7 to 40 kg/m^{2}s, and temperatures up to 400°C. Results have been obtained for two sizes of sand. The ratio of secondary to primary air has been varied from 0 to 1.5. These conditions are closer to industrial practice than conditions associated with previously reported data.

Experimental Equipment

The equipment used for these experiments is the pilot-scale CFB combustor recently constructed at the University of British Columbia. Figure 1 shows the major components of this unit. The fast bed section is 7.3 m high and 152 × 152 mm in cross-sectional area. Preheated primary air is introduced through a distributor plate with three tuyeres and six holes per tuyere at the bottom of the column. Secondary air is fed through two pairs of directly opposed air ports of 32 mm dia. located 0.9 m above the distributor plate, on two facing walls. Solids are returned to the column 0.4 m above the distributor plate from a standpipe of 0.10 m ID through an L-valve (Knowlton and Hirsan, 1978). The solid recirculation rate is controlled by varying the amount of aeration air to the L-valve.

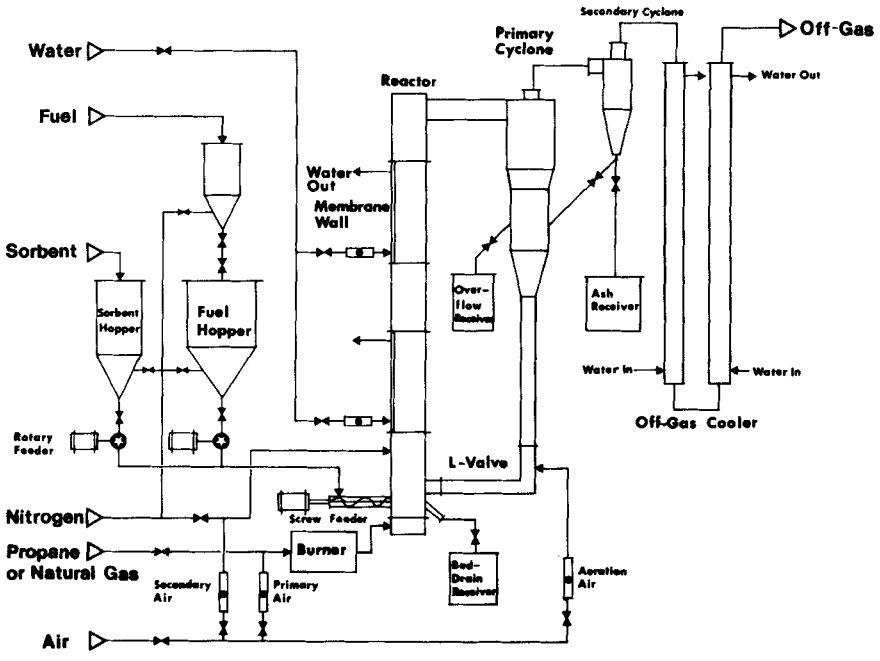

Figure 1. Pilot-scale circulating fluidized bed facility.

Solid particles entrained from the column are continuously captured by the primary cyclone, which returns the solids to a storage hopper connected to the standpipe. Most fine particles not captured by the primary cyclone are captured in a secondary cyclone. The gas stream is then vented after being cooled in an off-gas heat exchanger. The entire fast bed column (except for the membrane wall portions) and the primary cyclone are refractory-lined.

Although this unit is designed to run as a combustor for a variety of fuels, all results presented in this paper were obtained by operating the unit as a hot CFB, i.e., with no combustion in the reactor. A preheater burner that could be fed with either natural gas or propane was used to heat the unit. The CFB reactor is instrumented with thermocouples and pressure taps at 0.6 m intervals, shown in Figure 2, to monitor temperatures and suspension density profiles. Particles used in the present experiments were two Ottawa sands of 188 and 356 μm surface-volume mean diameter. Table 1 presents the key properties of these two sands.

Heat transfer data were obtained from two nearly identical heat transfer surfaces, each 1.53 m long and 148 mm wide, located on one wall of the column and beginning 1.22 and 4.27 m, respectively, above the distributor plate, Figure 2. Each surface consists of four identical, half-embedded, schedule 80 vertical stainless steel water-cooled tubes connected longitudinally by flat fins to form a membrane wall. Figures 3a and 3b show a plan view and a section view of the surfaces. The fins are flush with the refractory surface above and below. One of the central tubes in each surface is instrumented with eight thermocouples located approximately 150 mm apart. Temperatures and flow rates of water in turbulent flow inside the tubes are recorded. This enables one to calculate the average heat transfer coefficient (between thermocouples 1 and 8) or the heat transfer coefficient for the surface between any two thermocouples. For the conditions of the experimental study, the predominant heat transfer resistance is on the circulating bed side of the membrane surfaces. The resistance provided by the cooling water side has been estimated from the correlation of Sleicher and Rouse (1975). This resistance and that provided by the tube itself have been subtracted. The reported heat transfer coefficients are therefore bed-side (suspension to exposed surface)

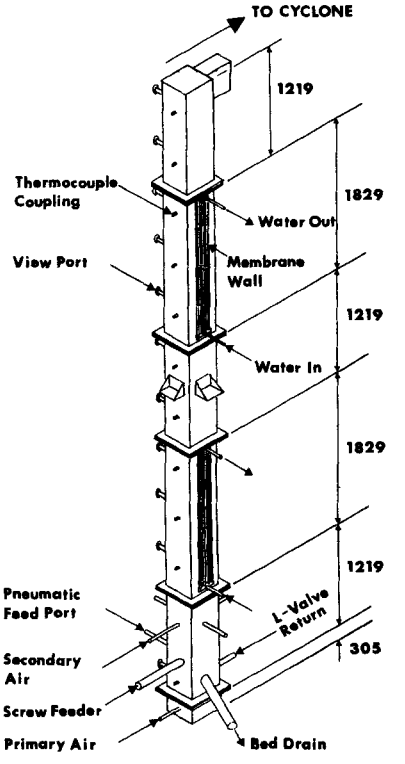

Figure 2. Principal reactor vessel: positions of heat transfer surfaces and thermocouples.

Pressure taps are at same heights as thermocouples, on opposite wall; dimensions in mm

Table 1. Particle Size Analyses and Fluidization Properties for the Two Sands

Size Range μm	Finer Sand wt. %	Coarser Sand wt. %
850–710	0.1	0.0
710–600	0.5	2.4
600–495	1.8	14.2
495–420	2.4	27.2
420–351	2.2	20.7
351–297	6.0	19.7
297–250	10.1	5.8
250–208	21.8	4.0
208–180	20.4	3.0
180–150	13.3	1.3
150–125	11.4	1.0
125–106	5.4	0.3
106–90	3.3	0.2
90–61	0.9	0.1
61–53	0.3	0.1
53–45	0.1	0.0
45–0	0.0	0.0
Sauter mean particle size, μm	188	356
Particle dens., kg/m³	2,637	2,642
Terminal settling veloc. at 300°C and 104 kPa, m/s	1.2	2.8
Min. fluidization veloc., mm/s	51	95
Voidage at min. fluidization	0.46	0.42

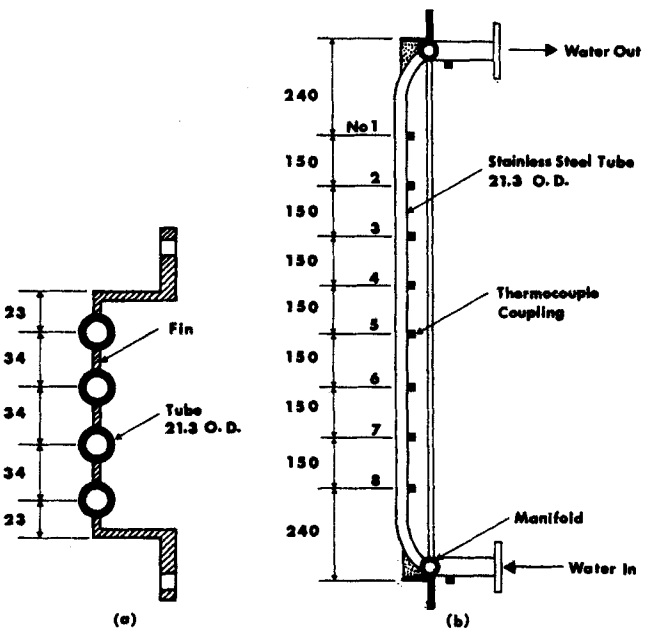

Figure 3. Membrane waterwalls used in heat transfer studies.
a. Plan view
b. Section view: position of thermocouples in membrane wall heat exchanger assemblies
Dimensions in mm

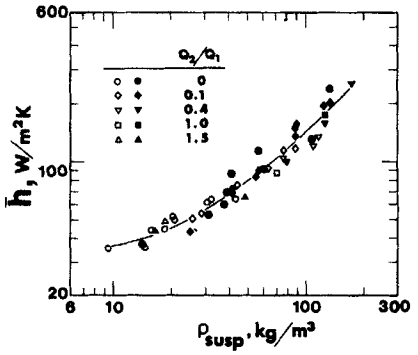

Figure 4. Average heat transfer coefficient for membrane wall surfaces as a function of suspension density, 188 μm sand.
Coefficients from thermocouples 1–8, Figure 3b
Open, filled symbols: upper, lower exchange surfaces, respectively

values. Heat transfer coefficients can be based on:

1. The exposed tube surface areas alone
2. The total projected surface area, or
3. The total of the exposed tube surface areas and the areas of the fins between the tubes

In the present paper, all reported coefficients refer to the last of these, i.e., the total exposed heat transfer area. To obtain coefficients based on the area 1 or 2, the coefficients reported here should be multiplied by 1.46 or 1.33, respectively. For an analysis of the effectiveness of the longitudinal fins as exchange surfaces, see Bowen et al. (1987).

Suspension densities reported here are cross-sectional area mean values estimated from measured pressure profiles. These are commonly used to infer suspension densities, with reasonable accuracy (Van Swaaij et al., 1970; Capes and Nakamura, 1973; Hartge et al., 1986).

Results and Discussion

Average suspension-to-surface heat transfer coefficients are plotted against the suspension densities in Figures 4 and 5 for sand particles of mean diameter 188 and 356 μm, respectively. The open and filled symbols respectively represent coefficients measured for the total upper and lower heat transfer surfaces. In

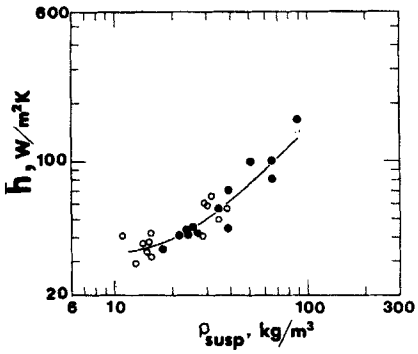

Figure 5. Average heat transfer coefficient for membrane wall surfaces as a function of suspension density, 356 μm sand.
Coefficients from thermocouples 1–8, Figure 3b
Open, filled symbols: upper, lower exchange surfaces, respectively
Secondary-to-primary air ratio = 0 in all cases

both cases, the heat transfer coefficient increases with suspension density. The two curves in Figures 4 and 5 for the two sands are almost identical, although the heat transfer coefficients for the larger sand appear to be somewhat lower at low suspension densities (<25 kg/m^3). There appears to be no systematic difference between the upper and lower exchange surfaces and no systematic influence of the secondary-to-primary air ratio.

The variation of the suspension-to-surface heat transfer coefficient as a function of superficial gas velocity for the 188 μm sand is shown in Figure 6. The lines drawn are least-squares regression lines for each value of suspension density. It is observed that superficial gas velocity does not significantly affect the heat transfer coefficient once the suspension density is established. This should not be surprising since the contribution of the gas convective component to the heat transfer coefficient is expected to be small compared to the particle convective component (Grace, 1986). One experimental point for no particles in the reactor is shown in Figure 6 for comparison. The measured heat transfer coefficient for this case, 18 W/m^2 · K, is in good agreement with published correlations, for example, that of Sleicher and Rouse (1975).

The influence of suspension temperature on the heat transfer coefficient is shown in Figure 7 for the 188 μm sand at three suspension densities, with the lines again corresponding to least-squares linear fitting. As for superficial gas velocity, the effect of suspension temperature on the heat transfer coefficient is minimal in the temperature range studied (150–400°C). The independent effects of superfical gas velocity, solids circulation rate, slip velocity, and suspension temperature were also observed to be very small for the 356 μm sand.

Analysis of heat transfer coefficients for part-lengths along the upper heat transfer surface shows that the coefficient decreased rapidly with decreasing height, with the maximum heat transfer coefficient occurring at the top of the surface in all cases. Figure 8a shows some typical profiles of the heat transfer coefficient as a function of height measured downward along the upper surface. The corresponding density profiles are also shown in Figure 8a. The trend is quite different for the lower heat transfer surface, as shown in Figure 8b.

The variation in coefficient over the upper surface suggests the existence of a layer of downflowing solids along the upper part of the combustor walls (and thus over the upper heat transfer surface), with fresh solids constantly coming into contact with the top part of the heat transfer surface and then traveling

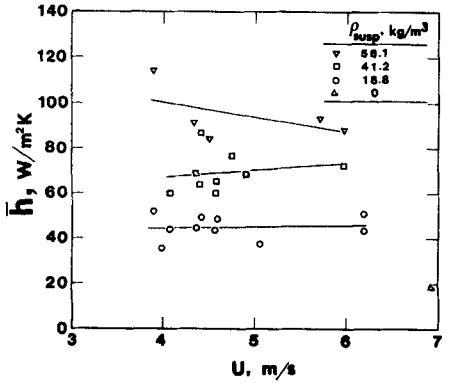

Figure 6. Influence of superficial gas velocity on average heat transfer coefficient, 188 μm sand.

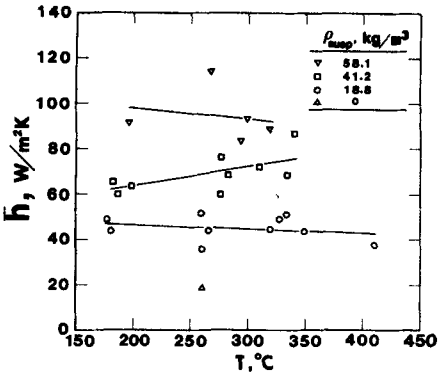

Figure 7. Influence of suspension temperature on average heat transfer coefficient, 188 μm sand.

down along the membrane waterwall surface. Existence of a predominantly downflowing layer of solids at the wall of a fast fluidized bed has been reported by Bierl et al. (1980), Weinstein et al. (1984), and Brereton and Stromberg (1986). The closeness of the slope values of the heat transfer coefficient profile lines to 0.5 in Figure 8a suggests that particle renewal in this layer of solids at the wall is minimal. The particle motion in the lower part of the bed is likely to be less regular than that on the upper surface, with particles moving sometimes upward and sometimes downward over the lower surface. Particle motions that are predominantly downward at the top but both upward and downward lower in the vessel are consistent with visual observations in a separate cold model CFB unit of 152 mm dia. in our laboratory. The up-and-down motion of particles passing over the lower heat transfer surface probably explains the minima in the heat transfer coefficient profiles observed at the middle of the lower surface. The increase in the suspension density over the lower part of the surface, Figure 8b, probably also contributes to the sharp increase in the heat transfer coefficient measured at the bottom of the lower surface.

Some discussion of the influence of the length of heat transfer surface is relevant here. The vertical length of heat transfer surfaces should be an important consideration in presenting heat transfer results for CFB units. This can be illustrated by comparing the present results, averaged over the length of the exchanger surfaces, with previously reported data in the literature (Mickley and Trilling, 1949; Kiang et al., 1976; Fraley et al., 1983; Kobro and Brereton, 1986). From Figure 9, it is apparent that the present results are significantly lower than the previous data for particles of comparable size. Also, very little influence of particle size is discernible in the present results. It should be noted, however, that all previous data (except for those of Mickley and Trilling, 1949) are local heat transfer coefficients measured using small heat transfer probes (e.g., water-cooled heat flux probe, electric heating element) with sizes of the order of centimeters. It seems likely that particle sheets of order 10–20 mm thick traveling past these small probes are far from achieving thermal equilibrium with the heat transfer surface, whereas particles passing along an extended surface, as in the present case, come close to reaching the surface temperature when they leave the surface and hence have a much lower driving force for heat transfer. Therefore, heat transfer measurements using short (and small) heat transfer probes result in significantly higher heat transfer coefficients than the much longer

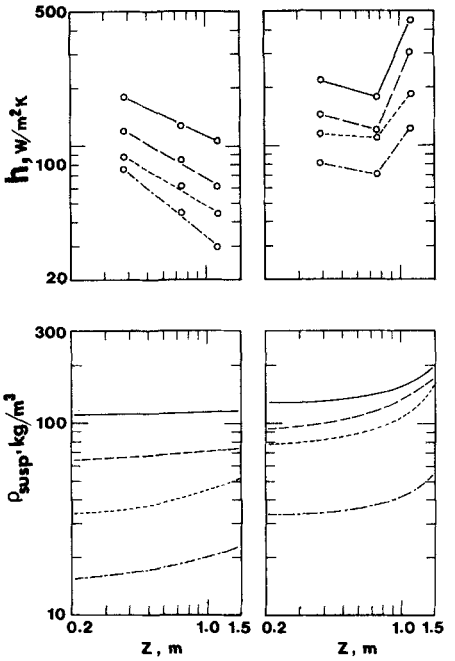

Figure 8. Typical longitudinal profiles of heat transfer coefficient and suspension density.

Coefficients obtained between thermocouples 1–3, 3–6, 6–8, Figure 3b

	Δp_R m H_2O	U m/s	T °C	G_s kg/m² · s	Q_2/Q_1
———	1.32	6.5	240	69	0.4
– – – –	1.20	5.6	190	28	1.0
·····	0.98	4.4	200	no data	0.0
—·—·—	0.39	4.4	333	no data	0.0

membrane walls in the present work. In addition, the influence of particle size becomes much less significant for longer surfaces since the residence time of particles at the surface is much longer than the particle thermal time constant for both small and larger particles. A secondary cause of the lower coefficients in the present work compared with previous studies is that the fins in our membrane walls are not as effective as an equivalent area of exposed tube surface (Bowen et al., 1987).

Figure 10 plots the heat transfer coefficient measured between thermocouples 1 and 3 at the upper surface vs. suspension density for both the 188 and the 356 μm sand. The local heat transfer coefficients between thermocouples 1 and 3 show more scatter but are generally higher than the average coefficients. Moreover, the particle size effect is more evident, with the smaller particles showing higher coefficients than the larger particles at the same suspension density. Thus, Figure 10 is in accord with the preceding discussion on the length of heat transfer surface. Figures 9 and 10 imply that CFB combustor designers should exercise caution when using available heat

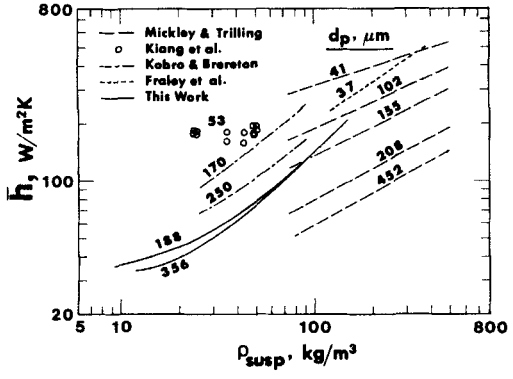

Figure 9. Comparison of heat transfer coefficients.

This work: 1.53 m long heat exchange surfaces
Heat transfer probe length, other studies: 880 mm (Mickley and Trilling), 57 mm (Kiang et al.), 150 mm (Fraley et al.), 100 mm (Kobro and Brereton)

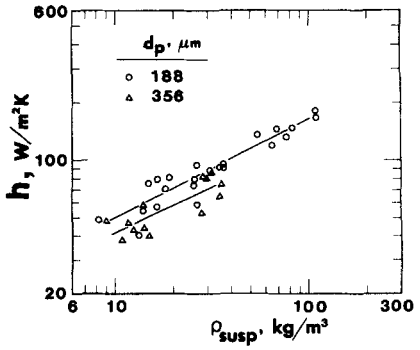

Figure 10. Heat transfer coefficient vs. suspension density for both sands.

Coefficient for section of upper heat exchange surface, thermocouples 1–3, Figure 3b

transfer data from the literature. As heat transfer surfaces in boilers tend to be long and in the form of membrane walls, underdesign is possible if local heat transfer coefficients obtained with miniature heat flux surfaces are used.

Conclusions

Suspension-to-surface heat transfer coefficients in circulating fluidized beds of sand are strongly influenced by the suspension density at that height, but only weakly influenced by superficial gas velocity (range 4–7 m/s), suspension temperature (range 150–400°C), and the ratio of secondary to primary air (range 0–1.5), once the suspension density is fixed. Heat transfer coefficients for the membrane waterwalls and the effect of particle size determined in the present work tend to be less than those reported in the literature by previous workers. This is primarily due to the much greater length of heat exchanger surface and the tendency of particles to move along the exchanger surface (downward along the upper surface, and both up and down along the lower surface). An understanding of particle motion is clearly essential to achieving a full understanding of suspension-to-surface heat transfer in circulating fluidized beds.

Acknowledgment

The authors are grateful to Energy, Mines, and Resources Canada and to the Natural Sciences and Engineering Research Council of Canada for financial support and to C. Brereton and E. J. Anthony for useful discussions.

Notation

d_p = surface-volume mean particle size
G_s = solids circulation flux
h = local suspension to tube-surface heat transfer coefficient
$\bar{h}$ = Average suspension to tube-surface heat transfer coefficient
Q_1 = primary air flow through distributor plate
Q_2 = secondary air flow
T = temperature
U = superficial gas velocity
Z = height measured downward from top of exposed heat transfer surface
Δp_R = total pressure drop over reactor
ρ_{susp} = suspension density averaged over reactor cross section

Literature Cited

Bierl, T. W., L. J. Gajdos, A. E. McIver, and J. J. McGovern, "Studies in Support of Recirculating Bed Reactors for the Processing of Coals," U.S. Dept. of Energy Rept. FE-2449 (1980).

Bowen, B. D., M. Fournier, and J. R. Grace, "Heat Conduction in Membrane Waterwalls," to be submitted to Int. J. Heat Mass Transfer (1987).

Brereton, C., and L. Stromberg, "Some Aspects of the Fluid Dynamic Behaviour of Fast Fluidized Beds," *Circulating Fluidized Bed Technology*, P. Basu, ed., Pergamon, Toronto, 133 (1986).

Capes, C. E., and K. Nakamura, "Vertical Pneumatic Conveying: An Experimental Study with Particles in the Intermediate and Turbulent Flow Regimes," *Can. J. Chem. Eng.*, **51**, 31 (1973).

Fraley, L. D., Y. Y. Lin, K. H. Hsiao, and A. Solbakken, "Heat Transfer Coefficient in Circulating Bed Reactor," ASME Paper No. 83-HT-92, Seattle (1983).

Grace, J. R., "Heat Transfer in Circulating Fluidized Beds," *Circulating Fluidized Bed Technology*, P. Basu, ed., Pergamon, Toronto, 63 (1986).

Hartge, E. U., Y. Li, and J. Werther, "Analysis of the Local Structure of the Two-Phase Flow in a Fast Fluidized Bed," *Circulating Fluidized Bed Technology*, P. Basu, ed., Pergamon, Toronto, 153 (1986).

Kiang, K. D., K. T. Liu, H. Nack, and J. H. Oxley, "Heat Transfer in Fast Fluidized Beds," *Fluidization Technology*, **2**, D. L. Keairns, ed., Hemisphere, Washington, D.C., 471 (1976).

Knowlton, T. M., and I. Hirsan, "L-Valve Characterized for Solids Flow," *Hydrocarb. Proc.*, 149 (Mar., 1978).

Kobro, H., and C. Brereton, "Control and Fuel Flexibility of Circulating Fluidized Beds," *Circulating Fluidized Bed Technology*, P. Basu, ed., Pergamon, Toronto, 263 (1986).

Mickley, H. S., and C. A. Trilling, "Heat Transfer Characteristics of Fluidized Beds," *Ind. Eng. Chem.*, **41**, 1135 (1949).

Sleicher, C. A., and M. W. Rouse, "A Convenient Correlation for Heat Transfer to Constant and Variable Property Fluids in Turbulent Pipe Flow," *Int. J. Heat Mass Transf.*, **18**, 677 (1975).

Van Swaaij, W. P. M., C. Buurman, and J. W. Van Breugel, "Shear Stresses on the Wall of a Dense Gas-Solids Riser," *Chem. Eng. Sci.*, **25**, 1818 (1970).

Weinstein, H., M. Shao, and L. Wasserzug, "Radial Solid Density Variation in a Fast Fluidized Bed," AIChE Ann. Meet., San Francisco (1984).

Manuscript received Jan. 9, 1987, and revision received Apr. 27, 1987.